Does Current Crowding Induce Vacancy Concentration Singularity in Electromigration?

Ozgur Taner, Kasemsak Kijkanjanapaiboon, and Xuejun Fan
Department of Mechanical Engineering
Lamar University
PO Box 10028, Beaumont, TX 77710, USA
Tel: 409-880-7792; xuejun.fan@lamar.edu

Abstract

Mathematical model of electromigration in terms of vacancy concentration is studied analytically and numerically in this paper with the combined effect of vacancy gradient (Fickian term) and electric flow. A 2-D, L-shaped, homogeneous material model with perfect blocking boundary condition (*J = 0*) is chosen as the problem of interest. Dandu and Fan have shown that current density singularity exists at the tip of the wedges when the angle $\theta_0 < 90°$ [13]. This study investigates the effect of current density singularity at the tip of the wedges towards the vacancy concentration at the same location. The results of the study, both analytically and numerically, show that the location of maximum vacancy concentration occurs at cathode side, but not at the location of current density singularity.

Introduction

Electromigration is a phenomenon of mass transport in electrical conductor under the driving force of electrical current. Open and/or short circuit in electronic devices are typical failures caused by electromigration due to voids nucleation near cathode side and hillock development near anode side. Several mathematical models have been proposed in order to understand and/or predict the electromigration [1-10]. They can also be utilized to improve the design of electronic devices in order to increase their reliability against electromigration failure [11]. Many studies employ the divergence as a metric for the failure, with four driving forces considered as the sources of electromigration failure. These four driving forces are vacancy concentration gradient (Fickian term), electric field or current, mechanical stress, and temperature gradient. In this paper, we consider electric field as the main driving force of electromigration failure, and the mathematical model of vacancy concentration coupling with electric potential is studied, analytically and numerically.

Dandu and Fan [12, 13] have shown that current density singularity, i.e. current crowding, exists at the tip of the wedges when the angles $\theta_0 < 90°$. Black has shown that the median time to failure due to electromigration is inversely proportional to the square of current density through experiments [1]. Based on this information, one might conclude that the location of maximum vacancy concentration would be at the location of current density singularity. In order to verify this statement, the vacancy concentration coupling with electric potential electromigration model is studied analytically and numerically. A 2-D, L-shaped, homogeneous material model with perfect blocking boundary condition (*J = 0*) is chosen to be the problem of interest because several electromigration experiments and/or observations are conducted under this configuration.

Mathematical Model

Electromigration is a phenomenon of mass transport, which can be described by Fick's diffusion equation as follows.

$$\frac{\partial C_v}{\partial t} = -\nabla \cdot J + G \tag{1}$$

where C_v is the vacancy concentration, J is the total vacancy flux, G is a generation or annihilation term. The total vacancy flux, J, is the sum of electromigration driving forces. The two driving forces, vacancy concentration gradient (J_1) and electric field (J_2), considered in this study can be expressed as follows.

$$J_1 = -D_v \nabla C_v \tag{2}$$

$$J_2 = -\frac{D_v C_v}{kT} Z^* e \nabla V \tag{3}$$

where D_v is the vacancy diffusivity, Z^* is the effective charge number, e is the elementary charge, V is the electric potential, k is the Boltzmann constant, T is the absolute temperature. Considering that the electrostatic potential must be equal to zero ($\nabla^2 V = 0$), then the governing equation for the two dimensional (2-D) vacancy concentration coupling with electric potential electromigration model in Cartesian coordinate system can be written as

$$\frac{\partial C_v}{\partial t} = D_v \left[\frac{\partial^2 C_v}{\partial x^2} + \frac{\partial^2 C_v}{\partial y^2} + \frac{Z^* e}{kT} \left(\frac{\partial C_v}{\partial x}\frac{\partial V}{\partial x} + \frac{\partial C_v}{\partial y}\frac{\partial V}{\partial y} \right) \right] \tag{4}$$

where the sink/source term $G = 0$ is used, which means grain boundary is not considered in this study, i.e. homogeneous material. In polar coordinate system, this governing equation can be written as

$$\frac{\partial C_v}{\partial t} = D_v \left[\frac{\partial^2 C_v}{\partial r^2} + \frac{1}{r}\frac{\partial C_v}{\partial r} + \frac{1}{r^2}\frac{\partial^2 C_v}{\partial \theta^2} + \frac{Z^* e}{kT} \left(\frac{\partial C_v}{\partial r}\frac{\partial V}{\partial r} + \frac{1}{r^2}\frac{\partial C_v}{\partial \theta}\frac{\partial V}{\partial \theta} \right) \right] \tag{5}$$

The boundary condition studied in this paper is perfect blocking boundary condition, where total flux equals to zero *(J = 0)*. Clement and Lloyd [3] call this boundary condition constant-volume boundary condition; it "corresponds to a situation where vacancies are conserved which could be maintained in a system where a thick strong passivation layer would preclude changes in the volume of the conductor."

$$J = J_1 + J_2 = 0 \tag{6}$$

The initial condition studied in this paper is

$$C_v(x,y,0) = C_{v0} \tag{7}$$

where C_{v0} is the initial vacancy concentration.

Analytical Solutions

In this section, the analytical solution to vacancy concentration (C_v) in polar coordinate system at the location of current density singularity is derived. Since our interest is to study vacancy concentration at the location of current density singularity, steady state solution ($\partial C_v / \partial t = 0$) is considered. In polar coordinate system, after applying the steady state condition, the governing equation (5) becomes

$$\frac{\partial^2 C_v}{\partial r^2} + \frac{1}{r}\frac{\partial C_v}{\partial r} + \frac{1}{r^2}\frac{\partial^2 C_v}{\partial \theta^2} + \frac{Z^* e}{kT}\left(\frac{\partial C_v}{\partial r}\frac{\partial V}{\partial r} + \frac{1}{r^2}\frac{\partial C_v}{\partial \theta}\frac{\partial V}{\partial \theta}\right) = 0 \tag{8}$$

For asymptotic solution, let electric potential *(V)* and vacancy concentration *(C_v)* be functions of r and θ as follows.

$$V(r,\theta) = r^{\lambda_1} \cdot f(\theta) \tag{9}$$

$$C_v(r,\theta) = r^{\lambda_2} \cdot g(\theta) \tag{10}$$

The schematic diagram of the analytical problem is illustrated in (Fig. 1).

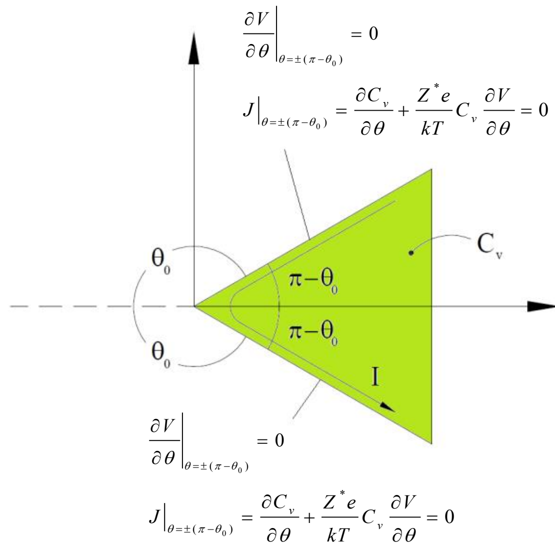

Figure 1. Schematic diagram of the analytical problem

According to Dandu and Fan [13], current density singularity occurs at the locations where $r \to 0$ and $\theta_0 < 90^\circ$. Their analytical solution to voltage function is

$$V(r,\theta) = f_0(\theta) + r^{\left[\frac{\pi}{2(\pi-\theta_0)}\right]} \cdot f_1(\theta) + r^{\left[\frac{\pi}{(\pi-\theta_0)}\right]} \cdot f_2(\theta) + r^{\left[\frac{3\pi}{2(\pi-\theta_0)}\right]} \cdot f_3(\theta) + \ldots \tag{11}$$

$$f(\theta) = A\cos\lambda(\theta) + B\sin\lambda(\theta) \tag{12}$$

Note that voltage function is expressed in series form, however, only the second term, which is $r^{\left[\frac{\pi}{2(\pi-\theta_0)}\right]} \cdot f_1(\theta)$, contributes to current density singularity $(\partial V / \partial r \to \infty)$. So, in order to study its effect towards vacancy concentration, we can simplify the voltage function to

$$V(r,\theta) \cong r^{\left[\frac{\pi}{2(\pi-\theta_0)}\right]} \cdot f_1(\theta) \tag{12}$$

Apply equations (10) and (12) into the governing equation (8), we have

$$r^{\lambda_2-2}\left[\lambda_2\left(\lambda_2 + \frac{\pi}{2(\pi-\theta_0)}\frac{Z^* e}{kT} r^{\left[\frac{\pi}{2(\pi-\theta_0)}\right]} f(\theta)\right) g(\theta) + \frac{Z^* e}{kT} r^{\left[\frac{\pi}{2(\pi-\theta_0)}\right]} f'(\theta) g'(\theta) + g''(\theta)\right] = 0 \tag{13}$$

Since the location of current density singularity is where $r \to 0$ and $\theta_0 < 90^\circ$, we find the term $r^{\left[\frac{\pi}{2(\pi-\theta_0)}\right]} \to 0$. Thus, the governing equation (13) can be reduced to

$$r^{\lambda_2-2}[g''(\theta) + \lambda_2^2 g(\theta)] = 0 \tag{14}$$

Next, we consider the self-diffusion of vacancy concentration under singularity analysis. Its governing equation in polar coordinate can be written as

$$\frac{\partial^2 C_v}{\partial r^2} + \frac{1}{r}\frac{\partial C_v}{\partial r} + \frac{1}{r^2}\frac{\partial^2 C_v}{\partial \theta^2} = 0 \tag{15}$$

By applying equation (10) into equation (15), we have the same result as equation (14), which indicating that current density distribution does not induce vacancy concentration singularity. We find agreement to this finding in the numerical study, as is discussed in the following section.

Numerical Solutions

To further investigate the 2-D electric field coupled vacancy concentration problem, the vacancy concentration equation is numerically solved using finite element method. Simulations are done in COMSOL Multiphysics software, with Free Equation modeling options COMSOL offers such as the "PDE Weak Form Subdomain" module. The problems are implemented by providing COMSOL, the domain and boundary integrals that construct the variational form equations. In this study, two problems are examined. Both of the problems are defined by identical governing equations including the boundary conditions imposed on the systems. However, the geometries of the problem domains are different; the first problem, a rectangular plane, and the second problem, an L-shaped line, respectively. In the first model, owing to the rectangular domain geometry, and the boundary conditions employed, an electric field occurs with the existence of only longitudinal electric potential gradient. Next, the second problem is considered, where current crowding is induced due to the L-shaped geometry.

Both numerical solutions belong to the vacancy transport equation with perfect blocking boundary conditions only with the contributions of two driving forces, vacancy gradient and electromigration force due to electric potential gradients. Diffusion coefficients in both problems are taken as constant.

In this work, normalized equations are taken into consideration. Therefore non-dimensional equations for the

Eq. (4), and electrostatic potential equation are derived. Normalized vacancy transport equation and Laplacian electric potential equations are written respectively as follows.

$$\frac{\partial C^*}{\partial \tau} = \frac{\partial^2 C^*}{\partial x^{*2}} + \frac{\partial^2 C^*}{\partial y^{*2}} + \frac{Z^* e}{kT} V_0 \left(\frac{\partial C^*}{\partial x^*} \frac{\partial V^*}{\partial x^*} + \frac{\partial C^*}{\partial y^*} \frac{\partial V^*}{\partial y^*} \right) \quad (16)$$

With normalized boundary conditions

$$J^* = -\left(\frac{\partial C^*}{\partial x^*} + \frac{\partial C^*}{\partial y^*} \right) - \frac{Z^* e}{kT} V_0 \left(\frac{\partial V^*}{\partial x^*} + \frac{\partial V^*}{\partial y^*} \right) C^* \quad (17)$$

And normalized electrostatic potential equation is written as:

$$\nabla^2 V^* = 0 \quad (18)$$

With Dirichlet boundary conditions, $V^* = 1$ and $V^* = 0$, at anode and cathode ends, respectively, and Neumann boundary conditions on the remaining boundaries. Normalized parameters are given as:

$$\tau = \frac{t}{t_c},\ t_c = \frac{D_v}{L_0^2},\ x^* = \frac{x}{L_0},\ y^* = \frac{y}{L_0},\ V^* = \frac{V}{V_0},$$

$$V_0 = \rho_0 j L_0, \text{ and } C^* = \frac{C_v}{C_{v0}}$$

Here, electromigration parameters are chosen in a similar manner that is introduced in Lloyd and Clement's paper [3]. In their work, coefficient in front of the electromigration force is suggested to be in a range of 2-8. In our simulation, a similar procedure is followed and the coefficient in front of the coupling terms of normalized vacancy and gradient of normalized electric potential is taken as, $\frac{Z^* e}{kT} V_0 = 1$.

Weak form equations of the normalized vacancy concentration and electrostatic potential equations derived to implement our model in COMSOL, which are used for both of the simulations, are written as:

$$\int_\Omega \frac{\partial C^*}{\partial \tau} \delta C^* d\tau = \int_\Omega \frac{\partial C^*}{\partial x^*} \delta\left(\frac{\partial C^*}{\partial x^*} \right) dA + \int_\Omega \frac{\partial C^*}{\partial y^*} \delta\left(\frac{\partial C^*}{\partial y^*} \right) dA$$

$$+ \int_\Omega \left(\frac{\partial C^*}{\partial x^*} \frac{\partial V^*}{\partial x^*} + \frac{\partial C^*}{\partial y^*} \frac{\partial C^*}{\partial y^*} \right) \delta C^* dA - \oint_\Gamma \frac{\partial C^*}{\partial x^*} \vec{n}\, \delta C^* ds$$

$$- \oint_\Gamma \frac{\partial C^*}{\partial y^*} \vec{n}\, \delta C^* ds \quad (19)$$

1. Solution of the First Problem

In this problem, vacancy concentration equation is coupled with electric potential equation with perfect blocking boundary conditions for both ends of the line, corresponding to anode and cathode. Other driving forces forged by mechanical stress gradient and temperature gradient are neglected. Simulation of this model basically yields the same results with the solution for the one dimensional vacancy transport equation driven by electromigration and diffusion with perfect blocking boundary conditions. Electromigration force is calculated coupling the electric potential gradients. Considering the Neumann boundary conditions and the shape of the line as illustrated in (Fig. 2), vertically constant distance between two boundary lines, electric potential gradients of only one direction will be effective on the electromigration force. Problem domain is modeled in COMSOL with a mesh consisting of 122 rectangular elements.

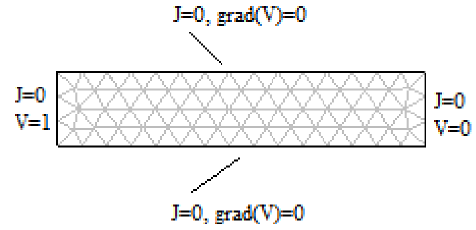

Figure 2. Mesh structure and boundary conditions

Results obtained by solving the Laplacian equation are shown in (Fig. 3). Gradients in vertical direction are not generated, thus reducing the problem to be 1-D in nature.

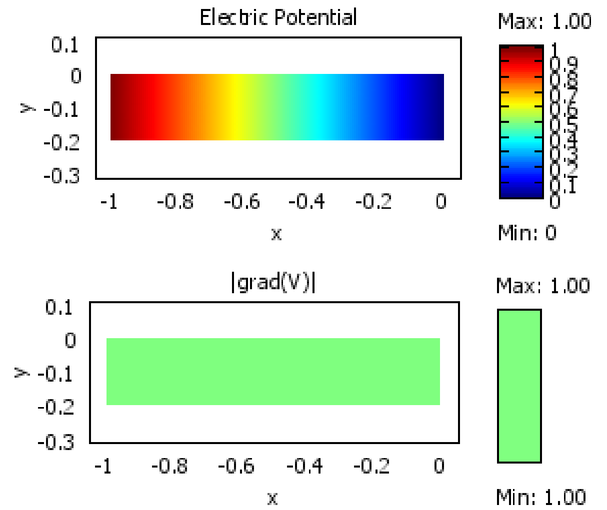

Figure 3. Electric Potential and Electric Field

This property enables the comparison of the simulation results with similar problems from literature. Additionally, an analytical solution is available in several published work for 1-D vacancy transport problems [9, 14], thus numerical results can be verified with exact solutions. In the end, a confirmation of the correct implementation of the equation is made before moving on to the more complex problem.

As expected, vacancy concentration increases at cathode end, referring to our model right end as shown in (Fig. 4). On the other hand, vacancy concentration decreases at left end, i.e. anode, and causes depletion in the vacancy. This is a natural result of the problem, mainly led by the electromigration force. Neumann boundary conditions employed for the solution of the electric potential equation on all the boundaries except at cathode and anode ends represent electric insulation, restriction of electron flow in this direction; thus, electric potential gradients perpendicular to the insulation boundaries will be zero. In the end, one dimensional electromigration force shifts the vacancy concentration balance in anode-cathode end direction, causing a higher

vacancy concentration on the cathode end, and the opposite on the other end.

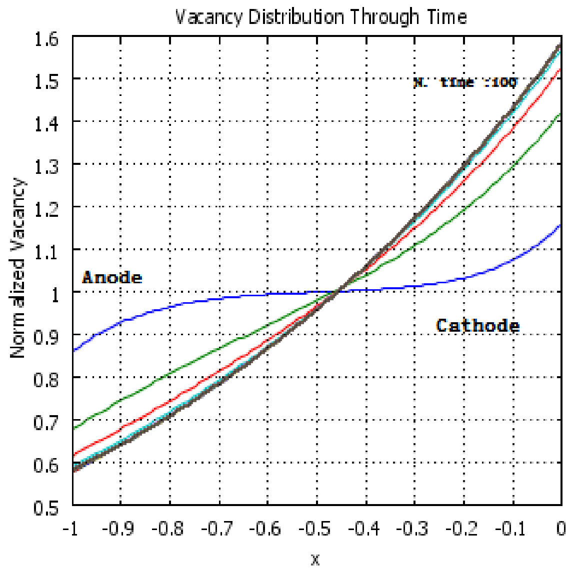

Figure 4. Vacancy concentration of the line at different time

2. Solution of the 2-D L-Shape Problem

In this problem, normalized vacancy concentration equation on an L-shaped geometry is studied. The main goal is to investigate the vacancy concentration, coupling with electric potential, which already shows singularity in its gradients due to current crowding effect, as discussed in the Analytical Solutions section. Here again, we take diffusion coefficient to be constant for entire domain, thus grain boundaries and vacancy sink/source terms are neglected. A schematic presentation of the problem with boundary conditions is given in (Fig. 5).

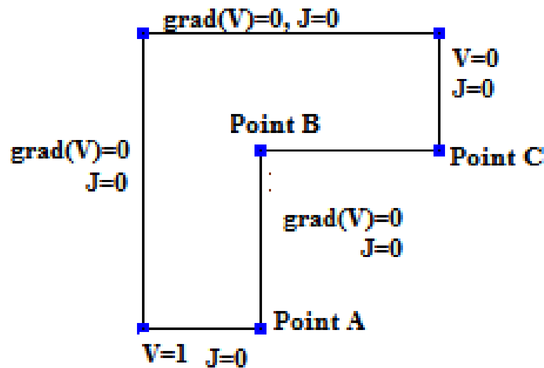

Figure 5. Problem geometry and boundary conditions

As illustrated in (Fig. 5), several locations are denoted as Point A, B, C, in order to be referred to when we investigate the vacancy concentration and electric field values.

Electric potential and electric field on the L-shaped geometry is illustrated in (Fig. 6). Electric field that is needed to compute electromigration force and the divergence of this force is obtained by solving electric potential equation with two Dirichlet boundary conditions at anode and cathode, and Neumann boundary conditions to maintain electric insulation on remaining boundaries.

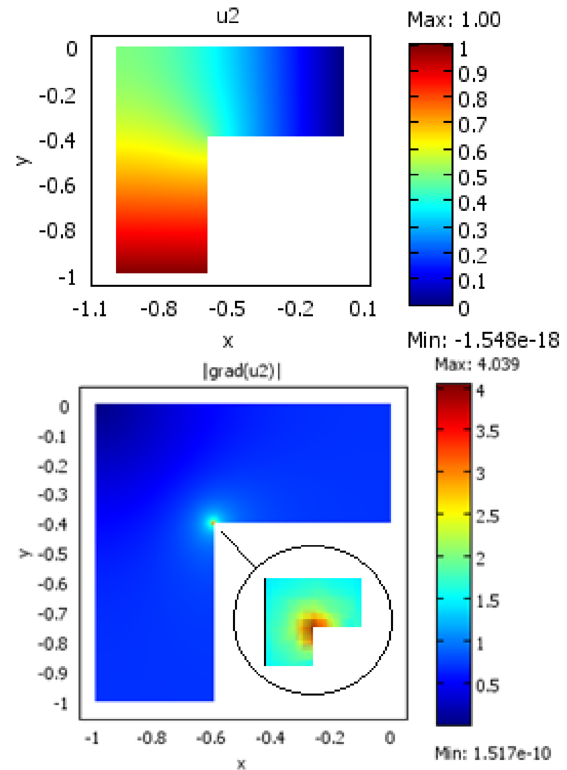

Figure 6. Electric potential and gradient

Electric gradient profile, on the L-shaped line, is found to be in agreement with analytical solution of Dandu and Fan [13], where singularity is observed for gradient of the voltage. Electric potential decreases from normalized value of one to zero, from anode end to the cathode end. Current crowding occurs at the corner on the path which electron flow follows.

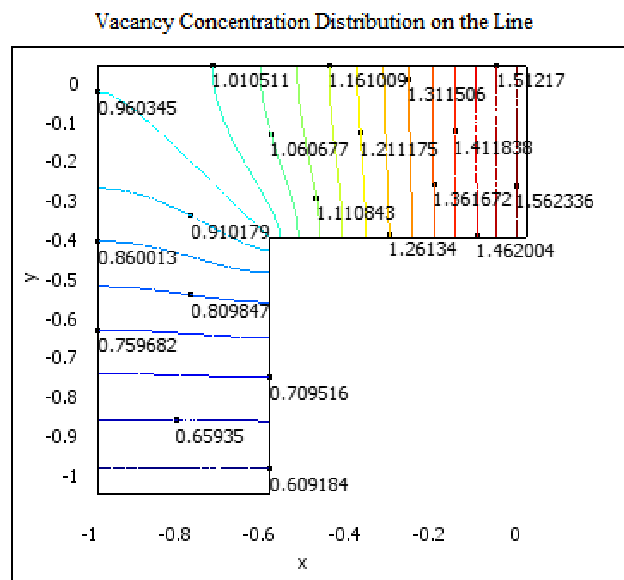

Figure 7. Vacancy concentration profile on the domain

Steady state solution of normalized vacancy concentration distribution along the L-shaped line is figured in (Fig. 7). Maximum vacancy concentration increases at Point C, located on the cathode end, where vacancy concentration decreases at Point A, i.e. anode, causing vacancy depletion. At Point B, where current singularity can be easily observed, vacancy concentration exhibits a lower value than the initial value. Vacancy concentration on the region surrounding this point remains mostly isometric, getting to the same steady-state vacancy concentration values.

Vacancy concentration values with the increasing time at the points of interest are figured in (Fig. 8). The results of our simulation comply with our analytical finding obtained by applying William's method [15] for solving singular stress field to our problem. It is observed that vacancy concentration does not show singularity where current singularity exists, nor is there an increased vacancy concentration on the surrounding region.

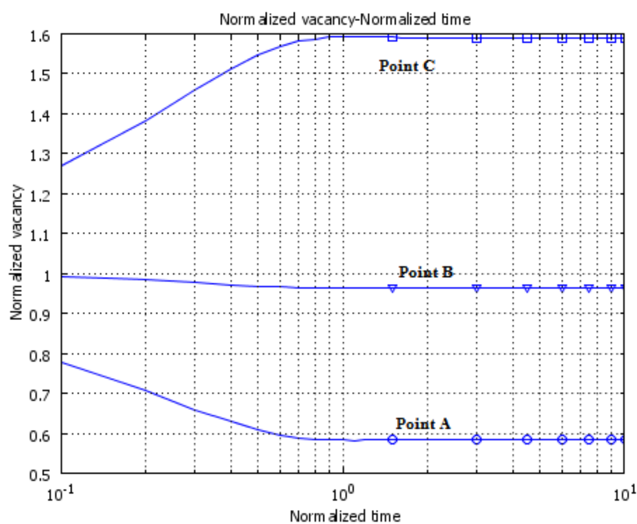

Figure 8. Vacancy progress with time at accumulation, depletion, and current crowding points

In the end, simulations show that, maximum vacancy concentration is located at the cathode end while vacancy depletion is seen at the anode side of the L-shaped line. With the increase in time, vacancy concentration increases at Point C, and decreases at points A and B. Vacancy concentration value is in a descendent regime even at Point B, where the magnitude of electric potential gradient becomes maximum, until problem enters the steady state.

Discussion

This study considers only two electromigration driving forces, vacancy concentration gradient and electric field. All other possible electromigration driving forces are excluded from this study. This is because electric field is considered the main driving force of electromigration failure, that is, without electric current there would be no electromigration failure. The solitary effect of electric field towards vacancy concentration, without distortion from other possible electromigration diving forces, is also a subject of interest. The results from this study can be used as a baseline to understand the effects of other electromigration driving forces should they be implemented into the model.

For homogeneous material with constant vacancy diffusivity and perfect blocking boundary condition, the results from both analytical and numerical study show that there is no indication of vacancy concentration singularity at the location of current density singularity. Instead, the location of maximum vacancy concentration is found to be at cathode side as shown in the numerical results. The experiment performed by Nemoto et al. [16] shows that, for conductor with passivation film, which is considered perfect blocking boundary condition in this study, voids accumulated at cathode side, but, for conductor without passivation film, generation and accumulation of voids was observed at the tip of the wedge. The study done by Zhang et al. shows that voids in solder joint generated at the location of current crowding [17]. At first, their results seem to be in contradiction to the results of this study, however, should the effects of two different conducting materials contacting each other and their interfacial boundary be considered, then the location of current crowding is also the location of cathode of the solder joint, where maximum vacancy concentration occurs.

Despite the agreement we find with other studies, voids accumulation due to electromigration do occur at the corner of L-shape interconnect structure as shown in the study published by He et al [6]. From our study, maximum vacancy concentration does not occur at the location of current density singularity, which means some other forces are likely in effect. The model proposed by Nemoto et al. shows that mechanical stress can shift the location of maximum vacancy concentration [16]. However, whether or not mechanical stress has any influence to the location of maximum vacancy concentration, this topic is to be discussed in another study.

Conclusion

The mathematical model of vacancy concentration coupling with electric potential is studied analytically and numerically. A 2-D, L-shaped, homogeneous material with constant vacancy diffusivity and perfect boundary condition is chosen as the problem of interest. Current density singularity is known to present at the tip of the wedge; however, the results from the study, both analytically and numerically, show that there is no vacancy concentration singularity at this location. The maximum vacancy concentration is found to be at cathode side, instead of the location of current density singularity.

References

1. J. R. Black, "Electromigration – A Brief Survey and Some Recent Results," *IEEE Transactions on Electron Devices*, vol. ED-16, no. 4, pp. 338–347, Apr. 1969.
2. I. A. Blech, "Electromigration in thin aluminum films on titanium nitride," *Journal of Applied Physics*, vol. 47, no. 4, pp. 1203–1208, Apr. 1976.
3. Clement and Lloyd, "Numerical investigations of the electromigration boundary value problem," *Journal of Applied Physics*, 71 (4), pp. 1729–1731, Feb. 1992.

4. Korhonen et al., "Stress evolution due to electromigration in confined metal lines," *Journal of Applied Physics*, 73 (8), pp. 3790–3799, Apr. 1993.
5. Filippi et al., "The effect of current density, stripe length, stripe width, and temperature on resistance saturation during electromigration testing," *Journal of Applied Physics*, vol. 91, no. 9, pp. 5787–5795, May 2002.
6. He et al., "Electromigration lifetime and critical void volume," *Applied Physics Letters*, vol. 85, no. 20, pp. 4639–4641, Nov. 2004.
7. Cacho et al., "Modeling of Electromigration Induced Failure Mechanism in Semiconductor Devices," *COMSOL Users Conference 2007 Grenoble*, Oct. 2007.
8. Zheng et al., "A 2-D mesoscopic model coupling mechanical and diffusion for electromigration in thin films," *Computational Materials Science*, 46, pp. 443–446, 2009.
9. Orio et al., "Physically based models of electromigration: From Black's equation to modern TCAD models," *Microelectronics Reliability*, 50, pp. 775–789, 2010.
10. Y. Zhang, Y. Liu, L. Liang, and X. J. Fan, " The effect of atomic density gradient in electromigration," *Int. J. Materials and Structural Integrity*, vol. 6, no. 1, pp. 36–53, 2012.
11. P. Dandu, X. J. Fan, Y. Liu, and C. Diao, "Finite element modeling on electromigration of solder joints in wafer lelvel packages," *Microelectronics Reliability*, 50, pp. 547–555, 2010.
12. P. Dandu, X. J. Fan, and Y. Liu, "Some Remarks on Finite Element Modeling of Electromigration in Solder Joints," *2010 Electronic Components and Technology Conference*, 2010.
13. P. Dandu and X. J. Fan, "Assessment of Current Density Singularity in Electromigration of Solder Bumps," *2011 Electronic Components and Technology Conference*, pp. 2192–2196, Jun. 2011.
14. S. R. De Groot, "THEORIE PHENOMENOLOGIQUE DE L'EFFT SORET," *Physica IX*, no. 7, pp. 699–708, Jul. 1942.
15. Williams M., "On the stress distribution at the base of a stationary crack," *Journal of Applied Mechanics*, 24, pp. 109–114, 1957.
16. Nemoto et al., "In-situ observation of electromigration failure in AlCuSi interconnects with a passivation film," *Strength, Fracture and Complexity 5*, pp. 97–107, Sep. 2007.
17. Zhang et al., "Effect of current crowding on void propagation at the interface between intermetallic compound and solder in flip chip solder joints," *Applied Physics Letters*, 88, pp. 012106-1–3, 2006.